*Tellus* (1983) *35A*, 39–50

# The atmospheric energy budgets over North America, the North Atlantic and Europe based on ECMWF analyses and forecasts

By HANNU SAVIJÄRVI[1], *European Centre for Medium Range Weather Forecasts, Reading, Berkshire RG2 9AX, England*

(Manuscript received November 27, 1981; in final form March 24, 1982)

ABSTRACT

The kinetic energy, sensible heat and latent heat budgets and the total energy balance of the earth–atmosphere system are studied over North America, the North Atlantic and Europe. The data consist of 1 year (December 1979–November 1980) of ECMWF initialized objective grid point $\sigma$-coordinate analyses and the ensemble of forecasts for day 3. The results quantitatively confirm the thermally direct meridional circulation over North America with generation of kinetic energy and adiabatic heating in the troposphere; kinetic energy and sensible heat are exported out of the region. The opposite holds for the North Atlantic area. The residuals of the energy budgets give a realistic approximation of the unresolved sub-grid scale processes (friction, diabatic heating, moisture sources/sinks) in the analysed data. Budgets from the forecast data reproduce the main features present in the analysed data, but also indicate some defects in the parameterization of the sub-grid scale processes in the ECMWF model. The analysed data, taking 4 analyses per day separately, exhibit diurnal variations, the magnitude of which is consistent with observed small diurnal wind variations. The total energy balance obtained for the 3 areas is reasonable and points to a considerable heat convergence in the North Atlantic ocean.

## 1. Introduction

The main purpose of this study is to present internally consistent areal energy budget calculations for some limited areas. Such calculations have been performed previously by, e.g. Kung (1967) and Holopainen and Eerola (1979) for kinetic energy and Hutchings (1957) and Rasmusson (1968) for humidity, using aerological observations. The present calculations are based on objectively analysed grid point data, which have been subject to normal mode initialization. This procedure was preferred to using raw upper air data so as to get a consistent data set; moreover, the advantageous properties of the staggered grid and conservative finite difference schemes originally developed for the ECMWF model could thus be employed for diagnostic purposes.

The vertical profiles of kinetic energy, sensible heat, latent heat and geopotential energy flux convergences and energy conversion terms are studied for 3 areas: North America, North Atlantic and Europe. The residuals needed for balance in the energy budgets give an estimate of sub-grid scale effects (dissipation, diabatic heating, moisture sources) with a space scale separation clearly defined by the grid size. One year of data (December 1979–November 1980) is used, and the separation of analyses at 00, 06, 12, 18 GMT gives the possibility of finding the thermal tide in the energetics. Results are also shown for the ECMWF numerical forecasts for day 3. The residuals in the forecast data are the net effect of the parameterizations of sub-grid scale processes in the ECMWF model. They are compared with the

[1] Present affiliation: Department of Meteorology, University of Helsinki, Hallituskatu 11–13, Helsinki, Finland.



0280-6495/83/010039-12$2.50/0 

residuals from the analysed data. All the calculations are for area- and time-averaged values; no partition into time-mean and transient eddy modes or area mean and deviations has been made.

This paper is an abbreviated version of a technical report (Savijärvi, 1981a). Some effects of the initialization on the energy budgets were reported in Savijärvi (1981b) based on January 1979 FGGE data. The ECMWF analysis system is briefly described in Section 2. The ECMWF model performance for medium-range weather forecasts was described by Hollingsworth et al. (1980) and some general circulation experiments with this model were presented in Tiedtke (1980).

## 2. Outline of the data-assimilation procedure

We give here a short outline of the analysis-initialization procedure, through which the observations were channelled at ECMWF in 1980. The ECMWF operational analyses are made in a 6-h data assimilation cycle handling observations within $\pm 3$ h as simultaneous. The background field for the analysis is provided by the ECMWF 6-h forecast, except above 50 mb, where persistence and climatology are used instead. The deviations of observations from the background fields (increments) are analysed at 15 pressure levels with a 3-dimensional multivariate optimum interpolation scheme which uses all the available GTS data inluding satellite information. Furthermore, the wind increments are subject to local non-divergence within each analysis ($6° \times 6°$ rectangular) subvolume and are kept in an approximate geostrophic balance with height increments in the extratropics. The wind divergence is thus due mainly to the divergence in the increments on scales larger than about 1000 km. The analysis scheme is described in more detail in Lorenc (1981).

In addition to the analysis of height and wind, a separate analysis of humidity is made. The analysed variable is the integrated water content enclosed between successive standard pressure levels. As with height and wind, the preceding 6-h forecast is used to provide a first guess field, with appropriate interpolations between pressure and $\sigma$-levels. The humidity analysis method uses a single weighted average technique which resembles optimum interpolation for each individual datum.

In the non-linear adiabatic normal mode initialization (Temperton and Williamson, 1979) the fields are interpolated to the ECMWF model grid on $\sigma$-levels and the time tendencies of the normal modes corresponding to fast gravity waves excited by advancing one time step with the adiabatic model are removed; the slow Rossby modes are preserved in the process. Wiin-Nielsen (1980) suggested that this procedure should produce more appropriate and consistent (initial) values of the atmospheric variables, in particular, velocity potential and vertical velocity, which are useful for diagnostic studies. However, as discussed in Temperton (1980) and Kanamitsu (1980), the adiabatic initialization reduces mean meridional circulation and wind divergence, especially in the tropics, and thereby zonal means of meridional and vertical transports are underestimated. On the other hand, the non-linear normal mode initialization is capable of producing realistic vertical velocity patterns in mid-latitude weather disturbances (Daley, 1980) and subjective inspection of ECMWF analyses suggests that the initialized vertical velocity fields are much more acceptable to a meteorologist than the locally noisy uninitialized vertical velocities. The initialized data should thus be useful for limited area budget studies in mid-latitudes.

## 3. Energy budget calculations

Kinetic energy, sensible heat and latent heat energy are the only important energy forms for the atmospheric large-scale flow. Using sigma coordinates, the budget equations for these 3 energy forms can be written in flux form for a unit mass of air:

$$p_s R_k = \frac{\partial}{\partial t}(p_s k) + \nabla_\sigma \cdot (p_s k \mathbb{V}) + \frac{\partial}{\partial \sigma}(p_s k \dot{\sigma}) + p_s \mathbb{V} \cdot (\nabla_\sigma \phi + RT \nabla_\sigma \ln p_s), \tag{1}$$

$$p_s R_T = \frac{\partial}{\partial t}(p_s C_p T) + \nabla_\sigma \cdot (p_s C_p T \mathbb{V}) + \frac{\partial}{\partial \sigma}(p_s C_p T \dot{\sigma}) - p_s \alpha \omega, \tag{2}$$

$$p_s R_q = \frac{\partial}{\partial t}(p_s L q) + \nabla_\sigma \cdot (p_s L q \mathbb{V}) + \frac{\partial}{\partial \sigma}(p_s L q \dot{\sigma}), \tag{3}$$

where $R_k$, $R_T$, $R_q$ are the net effects (sources) of all contributions not represented by the local change, flux convergences and adiabatic pressure variations. In the hydrostatic balance assumed in eqs. (1)–(3), the adiabatic conversion and generation of kinetic energy through the horizontal pressure gradient force are linked diagnostically through geopotential flux convergences

$$-p_s \mathbb{V} \cdot (\nabla_\sigma \phi + RT\nabla_\sigma \ln p_s) = -\nabla_\sigma \cdot (p_s \phi \mathbb{V}) - \frac{\partial}{\partial \sigma}\left(p_s \phi \dot{\sigma} + \phi \sigma \frac{\partial p_s}{\partial t}\right) - p_s \alpha \omega. \quad (4)$$

Here sigma $\sigma = p/p_s$ is the vertical coordinate (pressure normalized by the surface pressure), $u$, $v$, $\dot{\sigma} = \mathrm{d}/\mathrm{d}t$ are the three wind components, $T$, $q$, $\phi$ the temperature, humidity and geopotential, $k = \frac{1}{2}(u^2 + v^2)$ the kinetic energy of horizontal flow, $\alpha = RT/p$ the specific volume and $\omega = \mathrm{d}p/\mathrm{d}t$. Dividing eqs. (1)–(4) by $g$ gives the convenient unit of W m$^{-2}$ for all the terms.

In the following, the vertical profiles of the terms in eqs. (1)–(3) are presented averaged over a 1-year period and over 3 mid-latitude areas, determining the right-hand side terms from analysed (or forecast) wind, temperature and humidity grid point data. The left-hand side (residual) term consists then of sub-synoptic turbulent flux convergences and other irreversible effects. Specifically, $R_k$ is the kinetic energy dissipation through surface and internal friction, $R_T$ consists of radiative effects, latent heat release and turbulent heating and $R_q$ is the net effect of condensation and evaporation and turbulent flux convergences. If forecast data are used in eqs. (1)–(3), the residual is produced by the subgrid scale parameterization scheme of the particular model; the ECMWF scheme is described in Tiedtke et al. (1979).

The finite difference approximations of the energy eqs. (1)–(4), used in this study are described in Burridge (1979). They are based on the ECMWF adiabatic model equations in a staggered grid, where the wind component points are displaced with respect to temperature points (the Arakawa C-grid). This configuration of variables allows a relatively accurate calculation of divergence and vertical velocity. The relation (4) is accurate in the finite difference scheme, and since the flux divergences disappear in integrating the equations globally with appropriate boundary conditions, this ensures that the finite difference system conserves total atmospheric energy (=potential + kinetic) and moisture under adiabatic conditions (no external sources, i.e. $R_k = R_T = R_q = 0$). (The ECMWF model is actually using the equations of motion, where the present difference scheme for rotational terms conserves potential enstrophy in non-divergent flow but does not fully conserve energy.) The time change in eqs. (1)–(3) disappears in the 1-year time mean of analysed data except for the daily cycle, but not in the forecasts in which there may be systematic errors. For the forecasts, the time rate of change is calculated as a centred time difference over a 48-h period.

The vertically integrated continuity equation in the $\sigma$-system is

$$\frac{\partial p_s}{\partial t} = -\int_0^1 \nabla_\sigma \cdot (p_s \mathbb{V})\,\mathrm{d}\sigma, \quad (5)$$

where the boundary conditions $\dot{\sigma} = 0$ at $\sigma = 0$, $\sigma = 1$ have been used. The global mass of the atmosphere is conserved by the differencing scheme.

It was found that the ECMWF initialized analyses also conserve mass well locally, i.e. the time mean vertical integral of mass convergence vanishes over the 3 areas (except for the thermal diurnal tide), and no artificial correction for the mass balance, typically encountered with aerological data (O'Brien, 1970), is needed. However, this was not the case with the ECMWF forecast ensemble means, where the systematic error of the model shows up as local surface pressure change of the order of several millibars per day. The pattern of this systematic error is rather similar at all heights (Derome, 1981) and, in accordance with eq. (5), is consistent with a vertically constant large-scale divergence of the order of $10^{-8}$ s$^{-1}$. This "spurious" mass divergence is not important in kinetic or latent heat energy budgets but has to be considered for sensible heat.

The data consist of ECMWF analyses and forecasts for the year December 1979–November 1980 in a 1.875° geographical grid (N48). As discussed above, initialization reduced mean meridional circulation to a level where zonally averaged transports of temperature, humidity, etc. are strongly underestimated, especially in the tropics, so the budgets will be discussed only for 3 limited areas in the Northern Hemisphere. The areas, shown in Fig. 1, cover North America, the North Atlantic and Europe. The area averages shown are weighted sums of the terms calculated for all grid points within the area. For horizontal flux divergences, this gives the same result as line integration along the area boundaries (by Gauss's theorem) often used in aerological data studies. The analysis-initialization step should make data consistent in that the temperature (and thus geopotential), humidity and horizontal wind all contain only scales representable by the grid, and in that there is a clear scale separation between large-scale contributions and sub-grid scale, the net effects of which are represented by the residuals $R_k$, $R_T$ and $R_q$. This scale separation may be obscured in studies using aerological data.

### 3.1. *The kinetic energy budget*

Fig. 2 shows the kinetic energy budget terms (eq. (1)) for the 3 areas, taking the yearly mean of 4 analyses per day (00, 06, 12, 18 GMT). There are 1414 cases in all. The North American area is similar to the area Kung used in a series of articles on kinetic energy dissipation calculated as a residual from aerological data. The main features and numerical values of the terms in Fig. 2 are, for North America, very similar to Kung and Baker's (1975) annual mean values based on 5 years of data.

The upper tropospheric flow over the North American continent is a source of kinetic energy (positive generation) which is then exported horizontally, while the North Atlantic and European areas act as sinks for kinetic energy importing the loss from outside. The implied poleward mean ageostrophic wind in the confluent flow over North America and equatorward ageostrophic wind in the jet exit over the North Atlantic and Europe is in good agreement with Lau's (1979) work on the maintenance of the time mean flow during winter.

The residual term shows two maxima in all 3 areas, one at the 300 mb level and the other in the planetary boundary layer. The unphysical "negative dissipation" in the layer between 700 and 800 mb caused by the negative generation term is probably due to the initialization procedure (Savijärvi, 1981b). This phenomenon is more severe over ocean areas. The boundary layer dissipation values for the 3 areas are listed in Table 1 for annual mean and for seasons. The free atmosphere dissipation and its secondary maximum is larger over the Atlantic and European areas than over the North American continent. This agrees with Elsaesser's (1969) results for the turbulent dissipation in the free atmosphere above 850 mb. Based on wind variance statistics through Kolmogorov's turbulence theory, he obtained area averaged values of 2–3 W m$^{-2}$ over the Atlantic and 1–2 W m$^{-2}$ over North America.

Holopainen and co-authors (1973, 1979) have extensively studied the kinetic energy budget over Britain and northwestern Europe using aerological data. A persistent feature in these works has been the large negative kinetic energy generation not completely balanced by horizontal convergence of

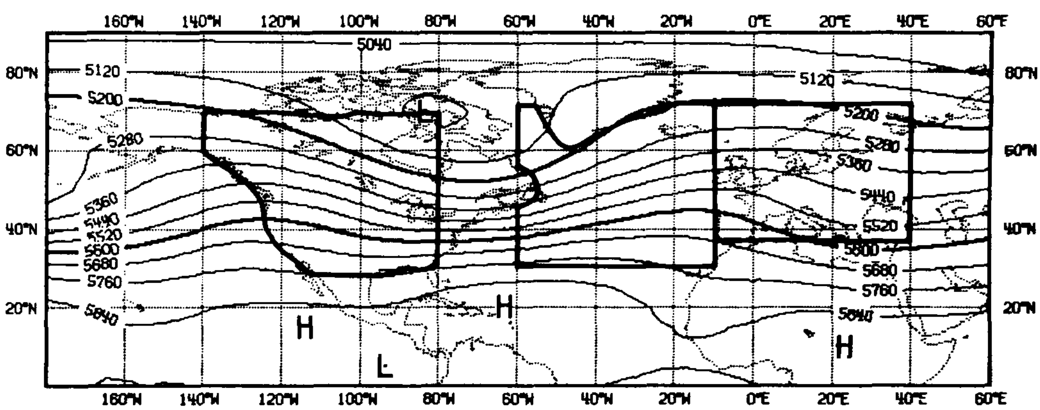


*Fig. 1.* Normal January 500 mb height contours and the 3 areas used for energy budget calculations.

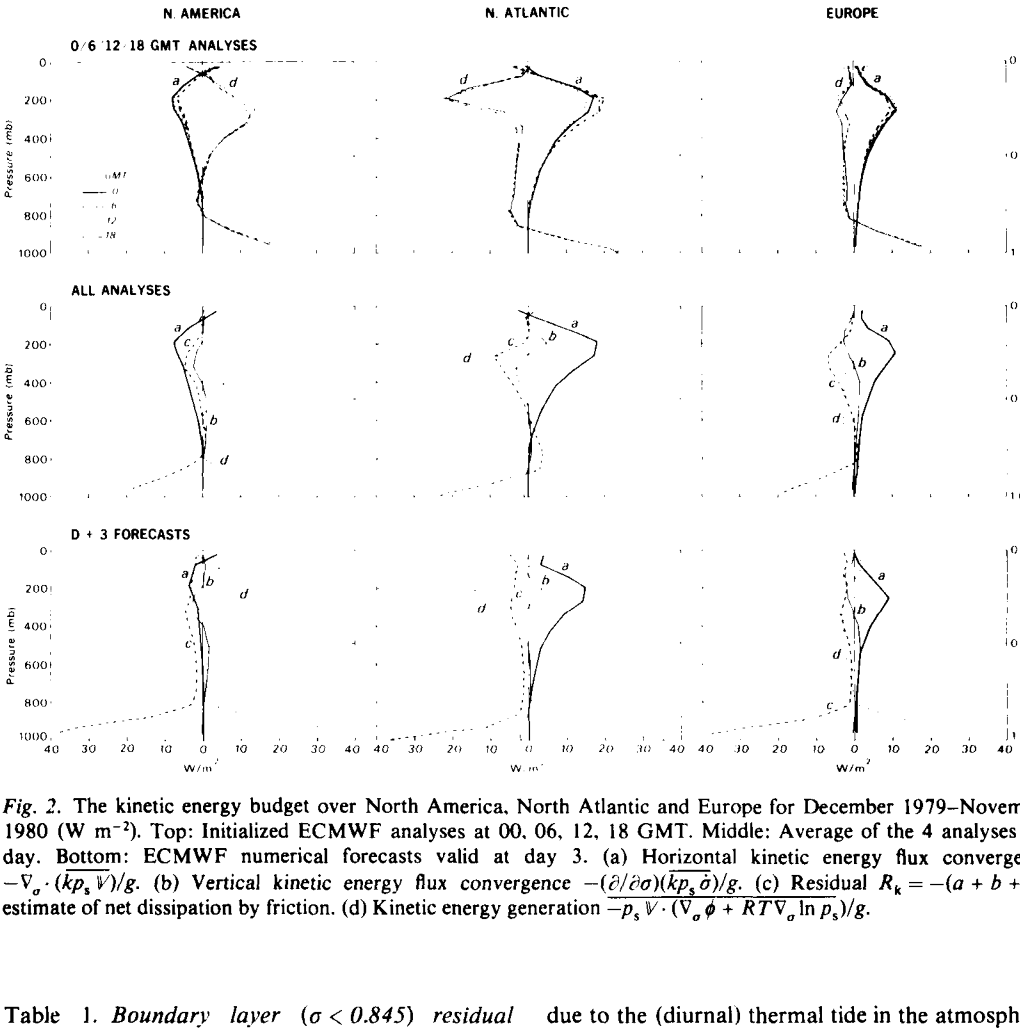


*Fig. 2.* The kinetic energy budget over North America, North Atlantic and Europe for December 1979–November 1980 (W m$^{-2}$). Top: Initialized ECMWF analyses at 00, 06, 12, 18 GMT. Middle: Average of the 4 analyses per day. Bottom: ECMWF numerical forecasts valid at day 3. (a) Horizontal kinetic energy flux convergence $-\nabla_\sigma \cdot \overline{(kp_s \mathbb{V})}/g$. (b) Vertical kinetic energy flux convergence $-(\partial/\partial\sigma)\overline{(kp_s \dot{\sigma})}/g$. (c) Residual $R_k = -(a + b + d)$; estimate of net dissipation by friction. (d) Kinetic energy generation $\overline{-p_s \mathbb{V} \cdot (\nabla_\sigma \phi + RT\nabla_\sigma \ln p_s)}/g$.

Table 1. *Boundary layer ($\sigma < 0.845$) residual dissipation from ECMWF analyses (W m$^{-2}$)*

| | Year | Spring | Summer | Autumn | Winter |
|---|---|---|---|---|---|
| North America | 1.5 | 1.6 | 1.0 | 1.6 | 1.9 |
| North Atlantic | 2.2 | 2.0 | 1.2 | 2.6 | 3.0 |
| Europe | 1.6 | 1.3 | 1.4 | 1.8 | 1.8 |

kinetic energy in the free atmosphere, which leads to positive residual values. This energy input from subgrid scales into the synoptic scale is contradictory to the present results. However, Holopainen's results are for much smaller areas.

The variation in Kung's (1967) results for 00 GMT and 12 GMT data taken separately was suggested by Wallace and Hartranft (1969) to be due to the (diurnal) thermal tide in the atmosphere. Fig. 2 presents the budgets for the ECMWF analyses separated to 00, 06, 12 and 18 GMT annual means. The diurnal variation in the kinetic energy budget terms over the North American area is similar to Kung's findings. Over the North Atlantic area the annual mean of kinetic energy generation is, at the 200 mb level, $-25$ W m$^{-2}$ in the 06 GMT analyses and $-21$ W m$^{-2}$ in the 12 GMT analyses. Assuming that the average geopotential gradient is equivalent to a constant westerly geostrophic wind of 20 m s$^{-1}$, this difference would suggest for the meridional wind component $v_{06\mathrm{GMT}} - v_{12\mathrm{GMT}}$ a value of 20 cm s$^{-1}$ from the south. This value is of the same order as that predicted by tidal theory (Chapman and Lindzen, 1970) for latitude 50° N. For observed lower stratospheric winds over England (100–150 mb; 8 observations per day) Johnson (1955) reported diurnal southerly winds $v_{06} - v_{12}$ of about 50 cm $s^{-1}$. The adiabatic initialization may, however, reduce the amplitude of the diurnal wind variation, because this variation is driven mainly by the purely diabatic direct absorption of solar radiation in ozone and water vapour through deep layers of the atmosphere.

The variation of the analysed wind speed within the 4 analyses per day is about 30 cm $s^{-1}$ at the 200 mb level over the 3 areas. That the systematic diurnal variation can survive initialization at all is interesting, because random variations, produced for a Monte Carlo forecast experiment, did not survive (Hollingsworth and Savijärvi, 1980), even if they were set into geostrophic balance with mass variations.

Fig. 2 also shows the kinetic energy budgets taking the annual mean of all ECMWF forecasts valid at day 3. There are 285 cases, as forecasts were not made during weekends for much of 1980. The small local decrease of kinetic energy at all levels in the kinetic energy during the forecast period is not included in Fig. 2 because it amounts only to about 0.1 W $m^{-2}$.

The boundary layer cross-gradient flow, which is responsible for the generation of kinetic energy, is stronger in the forecasts than in the initialized analyses. This is balancing the dissipation that results from the parameterization of turbulent momentum fluxes with the aid of mixing length theory in the ECMWF model. Initialization might reduce this diabatic dissipation in the analysed data, but as discussed in Temperton (1980) and Daley (1980), the reduction is probably small for this shallow-layer phenomenon. The boundary layer values in studies based on rawinsonde observations (Kung and Baker, 1975; Holopainen and Eerola, 1979) are, moreover, nearer to the analysed values than to the 3-day forecast values.

Above the boundary layer, the residual dissipation profile is vertically less variable and the secondary maximum is weaker in the forecast data than in the analysed data. The secondary maximum at the 300 mb level is qualitatively natural, due to strong winds, clear air turbulence and strong vertical wind shear at the jet level. Its relative weakness in the forecast data suggests that the dissipative mechanisms could be improved in the ECMWF model.

### 3.2. *The sensible heat budget*

The annual sensible heat budget is presented in Fig. 3, for the analysed and forecast data. The sum of the horizontal and vertical convergences of the sensible heat flux is shown, together with the adiabatic heating term and the residual $R_T$ needed to balance the time-averaged heat budget (eq. (2)). In the middle and upper troposphere, the continental regions (North America and Europe), located in the climatological jet entrance, are areas of heat flux divergence and adiabatic heating while the North Atlantic area, in the climatological jet exit, indicates heat flux convergence and adiabatic cooling. The magnitude of the diurnal variation in the $\alpha\omega$ and heat flux convergence terms deduced from the 4 daily analysed values in Fig. 3 amounts to about 50 W $m^{-2}$. As described in Section 3.1, the diurnal wind component may be underestimated in the ECMWF analyses after the adiabatic non-linear normal mode initialization, and the variation in the terms may be even larger in reality. The scatter in the 4 daily analyses ensemble means also serves to show the high sensitivity of the sensible heat budget calculations.

The residual profile from Fig. 3, interpreted as net diabatic heating, shows boundary layer heating, which amounts to about 120 W $m^{-2}$ or 1 °C $day^{-1}$ near the surface in all 3 areas. Over the ocean area, the heating extends through a deeper layer up to 500 mb; (radiative) cooling predominates in the upper atmosphere except in the stratosphere over North America. These features agree with estimates of diabatic heating by e.g. Lau (1979) and Clapp (1961) for the wintertime Northern Hemisphere; however, numerical values are smaller in the present study.

Fig. 3 also gives the ensemble mean of the sensible heat budgets calculated from all ECMWF 3-day forecasts for December 1979–November 1980. The model parameterization did not include the daily cycle. The local cooling present in the ECMWF model data is included as an extra curve in Fig. 3. Compared to the analysed data, the model residual indicates stronger but shallower boundary layer heating amounting to 150 W $m^{-2}$ or more at the surface in all 3 areas. The model data does not produce the extended heating in the lower troposphere over the North Atlantic. This indicates a relative weakness of simulated condensation processes over the ocean, presumably in the

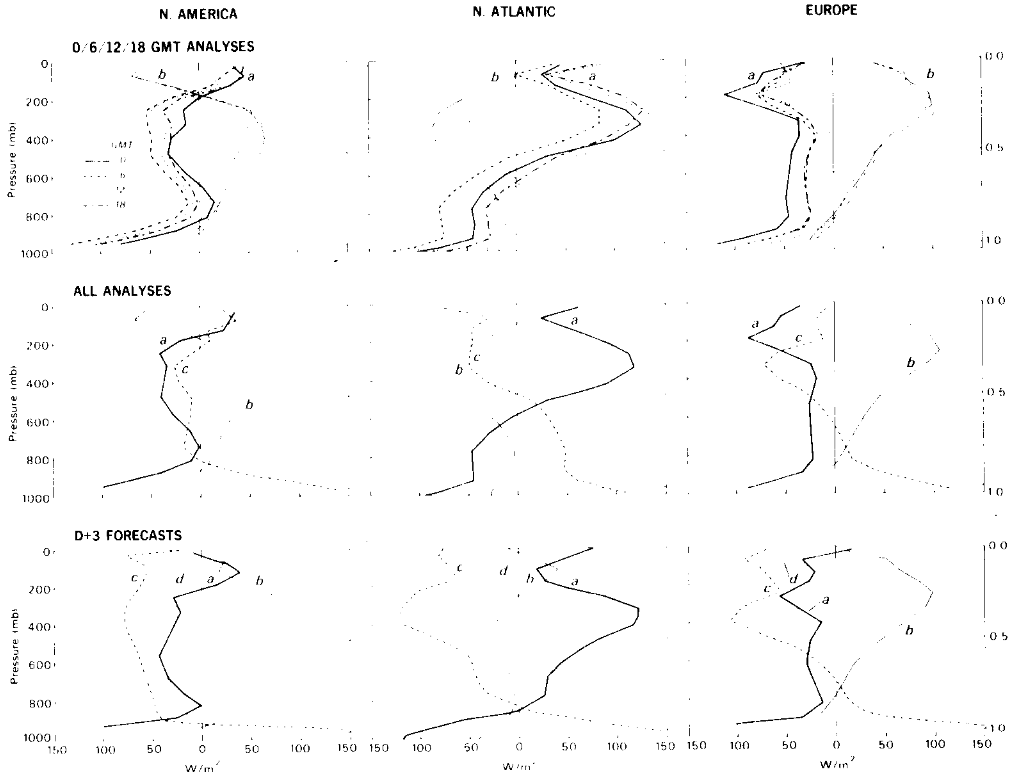


*Fig. 3.* As Fig. 2, but for the sensible heat budget (W m$^{-2}$); 1 °C/day ~115 W m$^{-2}$. (a) 3-dimensional heat flux convergence. (b) Adiabatic heating $\overline{p_s \alpha\omega/g}$. (c) Residual $R_T = -(a + b + d)$; estimate of net diabatic heating. (d) Local change $(p_s c_p \partial \bar{T}/\partial t)/g$ following the forecasts (negligible in the analysed data).

convective (Kuo) scheme during cold air outbreaks. The diabatic cooling in the upper troposphere and stratosphere is much stronger in the forecast data, especially at around the 80 mb level.

### 3.3. *The latent heat budget*

The humidity (latent heat) budget (eq. (3)) is rather simple for a long time mean: in each fixed air volume, the horizontal and vertical convergences of the time-mean humidity flux must be balanced by net sources or sinks. In grid point data, the sources and sinks include the subgrid scale flux convergences in addition to the time-mean condensation and evaporation within the volume. If vertically averaged, these amount to the evaporation minus precipitation (on the surface), and this loss (gain) in the total water content in the air column must be balanced by flux convergence (divergence) through the horizontal walls.

Fig. 4 shows the annual mean of the humidity budget averaged over the 3 areas where the net sources are represented by the residual needed to balance the horizontal and vertical large-scale flux convergences. All the 4 analyses per day are used. The humidity was actually analysed with the aid of observations only for the winter period (December 1979–March 1980). During April–November 1980, the initial humidity field, from which the ECMWF model started and which was also used in the present diagnostic calculations, was replaced by the 6-h forecast for humidity.

The boundary layer is a layer of vertical flux divergence; moisture is transported upward from the surface in large-scale eddies. In mid-troposphere, all the 3 areas accumulate moisture by both vertical and horizontal large-scale convergence, which is being removed (negative residual) presumably by condensation. In the

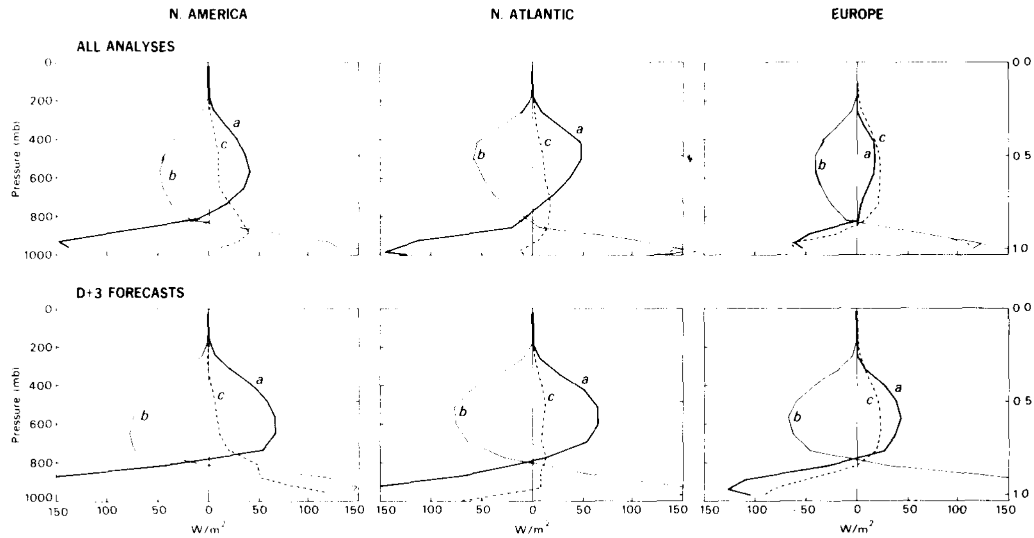


*Fig 4.* The latent heat energy budget over North America, North Atlantic and Europe for December 1979–November 1980 (W $m^{-2}$) 1 mm $H_2O$/day ~30 W $m^{-2}$. Top: average of 4 daily analyses. The diurnal deviation around the mean in the residual curve (b) is indicated by thin lines. Bottom: ECMWF numerical forecasts valid at day 3. (a) Vertical latent heat flux convergence $-(\partial/\partial\sigma)(\overline{Lqp_s\dot{\sigma}})/g$. (b) Residual $R_q = -(a + c)$; estimate of net moisture sources. (c) Horizontal latent heat flux convergence $-\nabla_\sigma \cdot (\overline{Lqp_s V})/g$.

boundary layer, there is net horizontal inflow of moisture over North America, while the net inflow is small over the North Atlantic (large inflow from west, but similarly large outflow in the east) and the European area indicates net horizontal outflow. The large positive residual needed to compensate the flux divergence in the boundary layer is due to evaporation from the surface, from falling precipitation, and from the net effect of (mainly vertical) convergence of humidity flux in small scale eddies. The 4 daily analyses are not presented, but the small diurnal variation in the residual is shown as the envelope curve made by all 4 daily analyses. Fig. 4 also shows the latent heat budgets for ECMWF day-3 forecasts. The local rate of change $\partial/\partial t\ (p_s Lq)$ amounts only to a few W $m^{-2}$ for the forecast data in Fig. 4 and is not included.

In the middle troposphere the horizontal flux convergence in the forecasts is similar to that in the analyses, but in the boundary layer it is enhanced. The large-scale vertical convergence is greatly enhanced through the whole column. This is an illustration of the "spin-up" problem; the (initialized) analysis does not provide a large enough correlation between humidity and vertical velocity, and it takes a few days for a model to reach its own circulation regime. Recent changes in the ECMWF analysis-initialization system have virtually eliminated the spin-up of condensation processes.

Table 2 lists the vertically integrated humidity flux convergences from Fig. 4 converted into cm $yr^{-1}$ of evaporation minus precipitation over the area.

Rasmusson (1968) has used aerological data to estimate evaporation minus precipitation (E − P) over U.S.A. and southern Canada for two 1-year periods. His results, which indicated an excess of precipitation of 16.0 and 18.8 cm $yr^{-1}$, are close to those obtained here. The diurnal variation (taking

Table 2. *Vertical integral of the humidity flux divergence in cm $yr^{-1}$ in ECMWF data for December 1979–November 1980*

| | All analyses | 3-day forecasts |
|---|---|---|
| North America | −13.4 | −19.7 |
| North Atlantic | −8.1 | −3.7 |
| Europe | −7.3 | −1.8 |

00 and 12 GMT observations separately) in Rasmusson's results was much larger than in the present results.

### 3.4. *The total energy balance of the earth–atmosphere system*

If the energy eqs. (1–4) are integrated vertically through an atmospheric column, and similarly, energy equations valid for the ocean-soil-cryosphere column are integrated from the surface down to the depth where the fluxes disappear, the sum is the equation for the total energy (Oort and Vonder Haar, 1976):

$$S_A + S_0 = -\nabla \cdot (\mathbb{F}_A + \mathbb{F}_0) + R_{ea} \quad (6)$$

of the earth–atmosphere system.

$S_A$ and $S_0$ are the local rates of change in the vertically integrated energy contents of the atmospheric and "oceanic" column (in the form of sensible heat, latent heat and kinetic energy for the atmospheric column). These storage terms disappear in a long time mean. Then, the time mean horizontal net energy flux divergence $\nabla \cdot (\mathbb{F}_A + \mathbb{F}_0)$ must balance the net energy flux $R_{ea}$ through the "vertical boundary"; $R_{ea}$ is physically the net radiation of the earth–atmosphere system at the top of the atmosphere and measurable by satellites. The vertically integrated flux of the total atmospheric energy $\mathbb{F}_A$ is, in $\sigma$-coordinates:

$$\mathbb{F}_A = \int_0^1 (c_p T + Lq + \phi + k) p_s \mathbb{V} \frac{d\sigma}{g}. \quad (7)$$

The wind in (7) can be either horizontal or 3-dimensional, because the vertical integration with the boundary conditions $\dot{\sigma} = 0$ at $\sigma = 0$, $\sigma = 1$ gives no net contribution from the vertical flux.

For zonally averaged conditions, Oort and Vonder Haar (1976) and Newell et al. (1974) have discussed the total energy budget. For limited areas there have been very few studies (cf. Alestalo, 1981), because of the large effect of wind divergence on the temperature and geopotential flux divergences and the difficulty in getting reasonable divergence values from observed winds.

The present results from ECMWF initialized analyses give the possibility of studying the total energy flux divergence $\nabla \cdot \mathbb{F}_A$ in the atmosphere over the 3 areas, North America, the North Atlantic, Europe. The North American area is land, where the horizontal fluxes $\mathbb{F}_0$ through the boundaries must be small: thus the net radiation $R_{ea}$ above this area should equal the atmospheric energy flux divergence in the long run. In the North Atlantic area, the heat flow in the ocean $\nabla \cdot \mathbb{F}_0$ may be large while the European area is partly land, partly sea.

In Fig. 5, the vertical profiles of the 4 atmospheric energy flux divergences are collected together. The divergences are 3-dimensional and the annual mean of initialized analysis calculations (4 analyses per day) is presented. It can be noted that near the surface the large positive sensible and latent heat divergences dominate the total energy. The kinetic energy flux divergence is relatively small everywhere. In the upper troposphere, the geopotential and sensible heat flux divergences are large but tend to balance each other. In the middle troposphere the latent heat flux convergence gives the largest contribution to the total flux divergence.

Fig. 5 also presents the divergence profiles for annual means of individual analysis 00, 06, 12, 18 GMT. The variability of geopotential and sensible heat flux divergence estimates suggested to originate from diurnal wind variations is obvious, while the latent heat and kinetic energy flux divergence calculations are less sensitive. (The diurnal wind speed is only about 30 cm $s^{-1}$ at the 200 mb level in the data.) This sensitivity and the tendency for balance between the 2 largest contributions means that the sum $\nabla \cdot \mathbb{F}_A$ of the vertical integrals of the 4 flux divergences must be considered with caution.

The annual area averages of the energy budgets are collected in Table 3, integrated vertically, taking the mean of all 4 analyses per day.

Estimates by Oort and Vonder Haar (1976) of the zonally averaged flux divergences in the mid-latitude belt 30–70° N give $-18$ W $m^{-2}$ for the atmospheric part $\nabla \cdot [\mathbb{F}_A]$ and $-22$ W $m^{-2}$ for the oceanic part $\nabla \cdot [\mathbb{F}_0]$; the net radiation $[R_{ea}]$ for this latitude belt is about $-40$ W $m^{-2}$ (Lorenz, 1967). The annual total energy flux divergences from the ECMWF analyses for the 3 limited areas in this latitude belt are thus reasonable, considering the sensitivity of the calculations, although the value for North America, $\nabla \cdot \mathbb{F}_A = -11$ W $m^{-2}$, is probably underestimated in magnitude. Maps of $R_{ea}$ from satellite measurements (Raschke et al., 1973) indicate that $R_{ea}$ does not vary much longitudinally

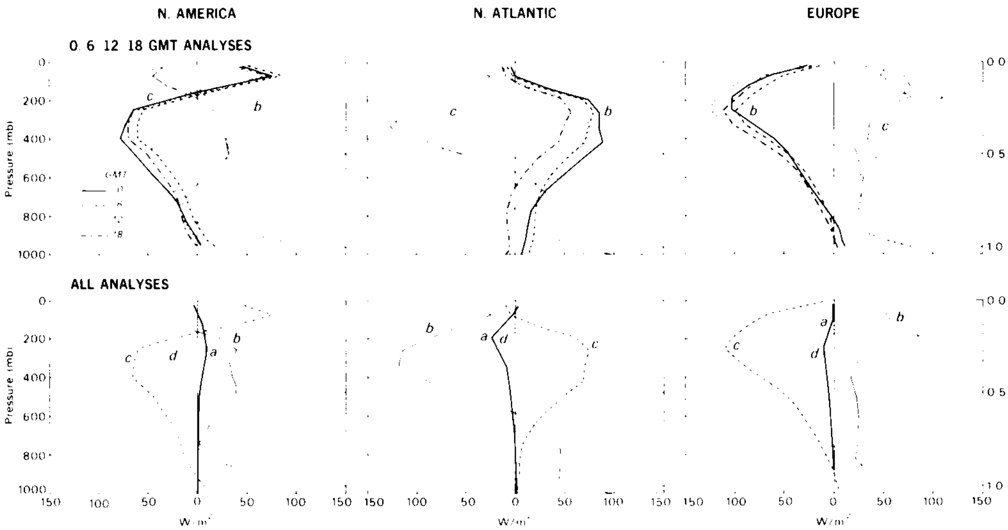


*Fig. 5.* The atmospheric 3-dimensional energy flux divergence profiles over North America, North Atlantic and Europe for December 1979–November 1980 (W m$^{-2}$). Top: initialized ECMWF analyses at 00, 06, 12, 18 GMT. Bottom: average of the 4 daily analyses. (a) Kinetic energy $\frac{1}{2}V^2$. (b) Sensible heat energy $c_p T$. (c) Geopotential energy $\phi$. (d) Latent heat energy $Lq$.

Table 3. *Vertically integrated annual energy budgets* (*W m*$^{-2}$)

*Sensible heat budget* (eq. (2))

| | $\mathrm{div}(c_p T \mathbb{V})$ | $-\alpha\omega$ | sum ≡ diabatic heating |
|---|---|---|---|
| Europe | 40.0 | −46.3 | −6.3 |
| North Atlantic | −21.6 | +27.5 | +5.9 |
| North America | 17.9 | −15.6 | +2.3 |

*Latent heat budget* (eq. (3))

| | $\mathrm{div}\,(Lq\mathbb{V}) \equiv L(E-P)$ |
|---|---|
| Europe | −6.1 |
| North Atlantic | −6.7 |
| North America | −11.0 |

*Kinetic energy budget* (eq. (1))

| | $\mathrm{div}\,(k\mathbb{V})$ | −generation | sum ≡ −dissipation |
|---|---|---|---|
| Europe | −3.6 | 0.6 | −3.0 |
| North Atlantic | −5.3 | 2.6 | −2.7 |
| North America | 2.2 | −4.5 | −2.3 |

*Energy flux divergences* div ($s\mathbb{V}$)

| | $s = c_p T$ | $Lq$ | $\phi$ | $k$ | sum $= \nabla \cdot \mathbb{F}_A$ |
|---|---|---|---|---|---|
| Europe | 40.0 | −6.1 | −45.7 | −3.6 | −15.4 |
| North Atlantic | −21.6 | 6.7 | 30.1 | −5.3 | −3.5 |
| North America | 17.9 | −11.0 | −20.1 | +2.2 | −11.0 |

around the zonal mean (−40 W m$^{-1}$) in these areas, so that the oceanic heat flow in the North Atlantic area must be large, because the atmospheric part $\nabla \cdot \mathbb{F}_A$ is small, −3.5 W m$^{-2}$. This area is in the middle of the Gulf Stream, so that large convergence of heat flux in the oceanic currents is expected.

Recent studies have stressed the rôle of oceanic heat transports also for the zonally averaged conditions (Vonder Haar and Oort, 1973). It may eventually be possible to geographically map the atmospheric heat flux divergences and to indirectly infer the ocean heat flux divergences with the aid of $R_{ea}$ measurements. Based on the present results, a good quality divergent wind field is needed for a reasonably accurate estimate of $\nabla \cdot \mathbb{F}_A$. Alestalo (1981) has calculated the total energy flux divergences using European aerological data for 3 years. His results give $\nabla \cdot \mathbb{F}_A = -55$ W m$^{-2}$ for continental Europe, which is reasonable, but this is arrived at with signs of sensible heat and geopotential flux divergences opposite to those presented in Table 3 for "Europe". The reason may be the smaller area in Alestalo's work; Europe is not clearly in a climatological jet entrance or exit and the choice of area may then have a drastic impact on the area-averaged energetics.

## 4. Concluding remarks

The present work is based on an extensive and good quality data set. It also includes diagnosis of forecast data. The results, the 1-year kinetic, sensible heat and latent heat energy budgets over North America, the North Atlantic and Europe, are in line with earlier results on the regional variations in the time-averaged energy equations based either on aerological data (e.g. Kung, 1967) or on (NMC) objective analyses (e.g. Blackmon et al., 1977; Savijärvi, 1977; Lau, 1979). According to the data, in the North America area (the climatological jet entrance) there is generation and horizontal flux divergence of kinetic energy and adiabatic heating and divergence of temperature flux in the middle troposphere. The North Atlantic (in the climatological jet exit) is an area of flux convergence and destruction of kinetic energy, adiabatic cooling and convergence of temperature flux, while Europe, not so clearly in a climatological jet entrance or exit, is somewhere between the two extremes. The results reveal a diurnal variation in the energy budget terms, presumably due to the thermal tide present in the initialized data. The magnitude of this variation is not inconsistent with observed diurnal wind variations.

The residuals of the energy budgets represent the expected sub-grid scale effects reasonably well. There is a sharp secondary dissipation maximum at the 300 mb level (as a residual) in all 3 areas. The boundary layer dissipation amounts to about 1.6 W m$^{-2}$ over the continental areas and 2.2 W m$^{-2}$ over the sea. The net heating (as a residual) is about 120–130 W m$^{-2}$ at the surface and the heating extends well into the middle troposphere over the ocean area.

The annual average of the 3-day forecasts from the ECMWF forecast model reproduces the main features in the analyses, but relative to the analyses reveals strong stratospheric cooling, strong and shallow boundary layer heating, not enough heating in the lower troposphere over the ocean area, spin-up of condensation processes, strong surface friction and a weak secondary dissipation maximum at the jet level.

The total energy balance of the earth–atmosphere system obtained for the 3 areas (as the sum of sensible, latent, kinetic and geopotential energy) is reasonable and points out the relatively large heat transport taking place in the ocean currents.

The good quality of the ECMWF initialized analyses, especially the divergent winds outside the tropics, has facilitated the qualitatively and quantitively coherent results presented here for mid-latitudes. It may even be possible to globally map the various atmospheric energy flux divergences, and as a by-product, the ocean flux divergences, once the remaining problem of weak tropical Hadley circulation resulting from adiabatic normal mode initialization is solved in the ECMWF analysis system. It may be speculated as to whether the residual studies should be based on observations rather than on objective analyses which were used in the present study. From the physical point of view, the objective analysis step may smooth out some features present in observations. On the other hand, a well-tuned analysis scheme increases the internal consistency and spatial coherence of data. From the modelling point of view, the present approach is useful in providing a verification of the parameterization scheme.

REFERENCES

Alestalo, M. 1981. The energy budget of the earth–atmosphere system in Europe. *Tellus 33*, 360–379.

Blackmon, M. L., Wallace, J. M., Lau, N.-C. and

Mullen, S. L. 1977. An observational study of the Northern Hemisphere winter time circulation. *J. Atmos. Sci. 34*, 1040–1053.

Burridge, D. 1979. Some aspects of large scale numerical modelling of the atmosphere. Seminars on dynamical meteorology and numerical weather prediction, September 1979, ECMWF, Reading, England.

Chapman, S. and Lindzen, R. S. 1970. *Atmospheric tides*. Dordrecht, Holland: D. Reidel Publ. Co.

Clapp, P. F. 1961. Normal heat sources and sinks in the lower troposphere in winter. *Mon. Wea. Rev. 89*, 147–162.

Daley, R. 1980. Normal mode initialization. Seminars on data assimilation methods, ECMWF Seminars, September 1980, Reading, England.

Derome, J. 1981. On the average errors of an ensemble of forecasts. ECMWF Tecnical Report No. 29.

Elsaesser, H-W. 1969. A climatology of Epsilon (atmospheric dissipation). *Mon. Wea. Rev. 97*, 415–423.

Hollingsworth, A., Arpe, K., Tiedtke, M., Capaldo, M. and Savijärvi, H. 1980. The performance of a medium range forecast model in winter. Impact of physical parameterization. *Mon. Wea. Rev. 108*, 1736–1773.

Hollingsworth, A. and Savijärvi, H. 1980. An experiment in Monte Carlo forecasting. Proceedings of the WMO symposium on probabilistic and statistical methods in weather forecasting, Nice, France, 45–47.

Holopainen, E. O. 1973. An attempt to determine the effects of turbulent friction in the upper troposphere from the balance requirements of large-scale flow: a frustrating experiment. *Geophysica 12*, 151–176.

Holopainen, E. O. and Eerola, K. 1979. A diagnostic study on the long-term balance of kinetic energy of the large-scale motion in the atmosphere over the British Isles. *Quart. J. Roy. Meteorol. Soc. 105*, 849–858.

Holopainen, E. O. and Nurmi, P. 1980. A diagnostic scale interaction study employing a horizontal filter technique. *Tellus 32*, 124–130.

Hutchings, J. W. 1957. Water-vapour flux and flux-divergence over southern England: summer 1954. *Quart. J. Roy. Meteorol. Soc. 83*, 30–48.

Johnson, D. H. 1955. Tidal oscillations of the lower stratosphere. *Quart. J. Roy. Met. Soc. 81*, 1–8.

Kanamitsu, M. 1980. Some climatological and energy budget calculations using the FGGE III-b analyses during January 1979. Seminars on data assimilation methods, September 1980, ECMWF, Reading, England.

Kung, E. C. 1967. Diurnal and long-term variations of the kinetic energy generation and dissipation for a five-year period. *Mon. Wea. Rev. 95*, 593–606.

Kung, E. C. and Baker, W. E. 1975. Energy transformations in middle-latitude disturbances. *Quart. J. Roy. Meteorol. Soc. 101*, 793–815.

Lau, N.-C. 1979. The observed structure of tropospheric stationary waves and the local balances of vorticity and heat. *J. Atmos. Sci. 36*, 996–1016.

Lorenc, A. C. 1981. A global three-dimensional multivariate statistical interpolation scheme. *Mon. Wea. Rev. 109*, 701–721.

Lorenz, E. N. 1967. The nature and theory of the general circulation of the atmosphere. WMO No. 218, TP. 115, Geneva, Switzerland.

Newell, R. E., Kidson, J. W., Vincent, D. G. and Boer, G. J. 1974. *The general circulation of the tropical atmosphere and interactions with extratropical latitudes*. Vol. 2. The MIT Press, 371 pp.

O'Brien, J. J. 1970. Alternative solutions to the classical vertical velocity problem. *J. Appl. Meteorol. 9*, 197–203.

Oort, A. H. and Vonder Haar, T. H. 1976. On the observed annual cycle in the ocean–atmosphere heat balance over the Northern Hemisphere. *J. Phys. Oceanogr. 6*, 781–800.

Raschke, E., Vonder Haar, T. H., Bandeen, W. R. and Pasternak, M. 1973. The annual radiation balance of the earth–atmosphere system during 1969–1970. From Nimbus 3 radiation measurements. *J. Atmos. Sci. 30*, 341–364.

Rasmusson, E. M. 1968. Atmospheric water vapor transport and water balance of North America. Large-scale water balance investigations. *Mon. Wea. Rev. 96*, 720–734.

Savijärvi, H. 1977. The interaction of the monthly mean flow and large-scale transient eddies in two different circulation types. Part II: Vorticity and temperature balance. *Geophysica 14* (2), 207–229.

Savijärvi, H. 1981a. The energy budgets in North America, North Atlantic and Europe based on ECMWF analyses and forecasts. Technical Report No. 27, ECMWF, 31 pp.

Savijärvi, H. 1981b. Energy budget calculations from FGGE analyses and ECMWF forecasts. Proceedings of the International Conference on preliminary FGGE data analysis and results, Bergen, Norway, 536–541.

Temperton, C. and Williamson, D. 1979. Normal mode initialization for a multilevel grid point model. ECMWF Technical Report No. 11, 99 pp.

Temperton, C. 1980. Design of the ECMWF normal mode initialization procedure. Seminars on data assimilation methods. ECMWF, 159–193.

Tiedtke, M., Geleyn, J-F., Hollingsworth, A. and Louis, J-F. 1979. ECMWF model-parameterization of sub-grid scale processes. ECMWF Technical Report No. 10.

Tiedtke, M. 1980. Diagnostics of diabatic processes in global numerical experiments at ECMWF. Proceedings of the Workshop: Diagnostics of diabatic processes, ECMWF, 135–152.

Von der Haar, T. D. and Oort, A. H. 1973. New estimate of annual poleward energy transport by Northern Hemisphere Oceans. *J. Phys. Oceanogr. 3*, 169–172.

Wallace, J. M. and Hartranft, F. R. 1969. Diurnal wind variations, surface to 30 km. *Mon. Wea. Rev. 97*, 446–455.

Wiin-Nielsen, A. 1980. Normal mode initialization—a comparative study. ECMWF Lecture Note No. 1.